

# Hollow to bamboolike internal structure transition observed in carbon nanotube films

Y. Y. Wang, S. Gupta,<sup>a)</sup> and R. J. Nemanich<sup>b)</sup>

*Department of Physics, North Carolina State University, Raleigh, North Carolina 27695-8202*

Z. J. Liu and L. C. Qin

*Department of Physics and Astronomy, University of North Carolina, Chapel Hill, Chapel Hill, North Carolina 27599-3255*

(Received 29 December 2004; accepted 10 May 2005; published online 8 July 2005)

The transition of the internal structure in microwave chemical-vapor-deposited carbon nanotubes is investigated using scanning electron microscopy and high-resolution transmission electron microscopy. By controlling the thickness of the iron catalyst layer, a sequence of carbon nanotube films was obtained with diameters ranging from a few nanometers to over 100 nm. Experiments have established that by continuous reduction of the Fe layer thickness to  $<1$  nm, single- and double-wall carbon nanotube films can be produced, whereas for an Fe film thickness  $>1$  nm, multiwall carbon nanotube films can be synthesized. It was also found that for an Fe thickness  $\geq 5$  nm, interlayers (i.e., bamboolike or periodically compartmentalized nanotubes) were formed, while for an iron thickness  $<2$  nm the tubes were primarily hollow. For an intermediate Fe thickness the internal structure of the carbon nanotubes was a mixture of hollow and bamboolike. A growth model which considers bulk and surface diffusions of carbon into and/or onto the Fe catalyst surface is proposed to describe this transition and the internal periodic structure. © 2005 American Institute of Physics. [DOI: 10.1063/1.1946198]

## I. INTRODUCTION

Carbon nanotubes (CNTs), one of the nanobuilding block candidates, have attracted a great deal of attention due to their unique structural, mechanical, chemical, and electronic properties.<sup>1</sup> In particular, small-diameter CNTs (i.e., single and double walled) ranging from 1 to 5 nm demonstrate either semiconducting or metallic properties depending on their chiralities and diameters,<sup>2</sup> which opens up the possibility of replacing silicon with CNTs in nanoelectronic devices. In addition to their applications in nanoelectronics, CNTs have also exhibited great potential for nanoelectromechanical systems (NEMSs),<sup>3</sup> biological sensors,<sup>4</sup> and electron field emission where carbon nanotube films are able to deliver a relatively high emission current (or current density) for a low average field.<sup>5</sup>

To meet the demands of the above-mentioned applications, high-quality CNTs with optimized growth in terms of diameter (small versus large), length (short versus long), orientation (vertical versus horizontal), chirality (semiconducting versus metallic), and purity are necessary and, in this respect, a fundamental understanding of the growth mechanism becomes important.<sup>6</sup> Pulsed laser vaporization (PLV) and electric arc (EA) discharge techniques are commonly used for mass production of CNTs. However, chemical-vapor deposition (CVD) is becoming an important approach because it enables nanotubes to grow directly on the substrates, and the growth can be controlled by variation of the deposition parameters.

In this paper, we report diameter-controlled CNT growth via microwave plasma chemical-vapor deposition (MWCVD).<sup>7</sup> Vertically aligned CNT (VACNT) films with CNT diameters ranging from a few to a hundred nanometers were obtained. Through continuous reduction of the catalyst layer thickness to 0.3–0.5 nm along with fast growth at a high deposition temperature, films of single- and double-wall CNTs with an areal density of  $\sim 10^{12}/\text{cm}^2$  have been achieved. Moreover, an internal structure transition from hollow to bamboolike has been observed.

Multiwall carbon nanotubes (MWNTs) deposited via MWCVD often exhibit a “bamboolike” structure. The origin of this periodic structure has long been debated and its implication to the growth mechanism is equally important. It has been suggested that the bamboo structures might be due to effects related to the (i) catalyst particle shape and/or size,<sup>8,9</sup> (ii) the displacement of the catalyst compared to the growth rate of the CNTs,<sup>10</sup> and (iii) bulk diffusion of carbon in the catalyst.<sup>11</sup> In this study, we systematically prepared films with CNTs which ranged from a few shells to a large number of shells, and we observed a transition of the internal structure. The results show that the internal structure closely correlates with the catalyst particle size, and we propose that the effect is related to the competition between surface and bulk diffusion. A growth model based on surface and bulk diffusion is used to explain the hollow to bamboo transition in nanotubes. Lastly, we also suggest that for small-diameter CNTs, surface diffusion predominates and becomes the major contribution for the nanotube growth.

<sup>a)</sup>Present address: Department of Physics and Materials Science, SW Missouri State University, Springfield, MO 65804-0027.

<sup>b)</sup>Electronic mail: robert\_nemanich@ncsu.edu

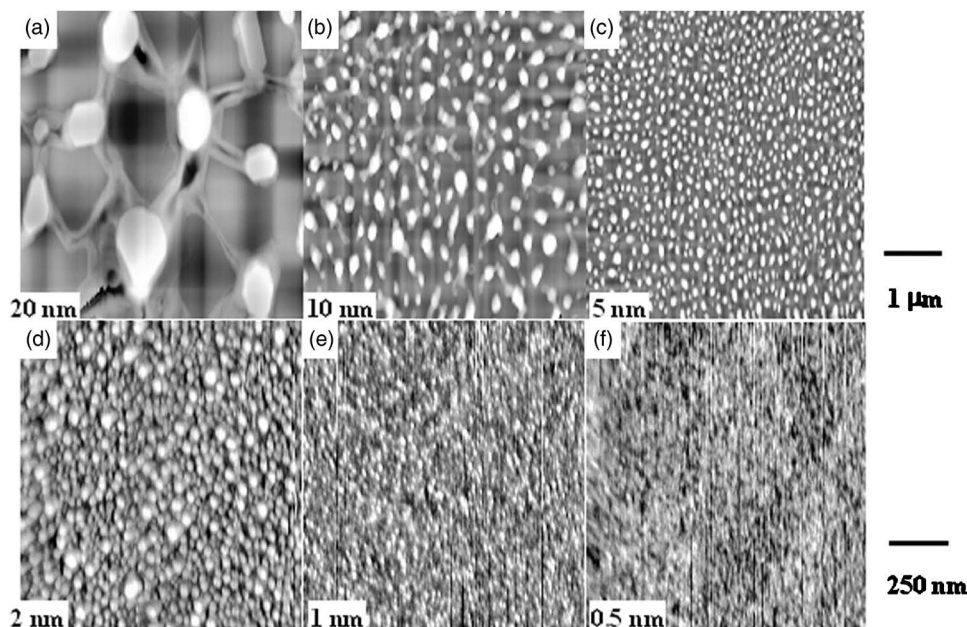


FIG. 1. Atomic force microscope images of annealed Fe on  $\text{SiO}_2/\text{Si}$  as a function of the Fe layer thickness. Note that the scale bar is  $1 \mu\text{m}$  for (a), (b), and (c) and  $250 \text{ nm}$  for (d), (e), and (f). Scans (e) and (f) are high gain and the system noise limits the image quality.

## II. EXPERIMENTAL DETAILS

The carbon nanotube films were grown in an ASTEX MWCVD system with microwave frequency of 2.45 GHz and a maximum output power of 1500 W. The same chamber has been used to grow polycrystalline diamond thin films.<sup>12</sup> Commercial Si (100) wafers were used as substrates, the wafers were first cleaned in JTB-100 for 15 min to remove surface particles and then rinsed in de-ionized water. Thermally grown  $\text{SiO}_2$  of 180-nm thickness was used as a buffer layer to prevent the catalyst layer from diffusing and interacting with the silicon and forming a silicide. The catalyst used was iron with different thicknesses (from 0.3 to 20 nm) deposited by e-beam evaporation, and the thickness was monitored by a quartz-crystal oscillator. The substrates were then transferred *in situ* into another UHV chamber with base pressure  $<10^{-9}$  Torr and annealed at  $850^\circ\text{C}$  for 10 min. Finally, the substrates were loaded into the MWCVD reactor for CNT growth. The MWCVD chamber was first pumped to  $10^{-3}$  Torr by a mechanical pump. A rf substrate heating source was turned on, and the temperature was ramped to  $650^\circ\text{C}$  before the gases were admitted into the chamber. The hydrogen ( $\text{H}_2$ ), with a flow rate of 200 SCCM (standard cubic centimeter per minute), was then introduced into the chamber to ignite the plasma. Once the plasma was turned on, the hydrogen was immediately closed and ammonia ( $\text{NH}_3$ ) and acetylene ( $\text{C}_2\text{H}_2$ ) in a 4:1 ratio were introduced into the reactor with flow rates of 70 and 18 SCCM, respectively. The substrate temperature was maintained at  $\sim 850^\circ\text{C}$  with heating from both the plasma and the induction heaters. Chamber pressure and plasma power were kept constant at 20 Torr and 600 W, respectively, and the growth time was from 30 to 90 s.

The nanotube film growth was carried out under a “bridge” configuration where two Si wafer sections were used as the supports, and another Si wafer section was used to bridge the two supports. The catalyst-covered substrate was positioned partially or fully beneath the bridge, which

served to screen the substrate from the plasma. The nanotube deposition took place underneath the covered regions. We presume that the Si wafer bridge serves to screen the growing CNT from the ions and atomic hydrogen in the plasma.

The as-deposited films were characterized by scanning electron microscopy (SEM) (Model JEOL 6400F), high-resolution transmission electron microscopy (HRTEM) (JEOL 2010F), and Raman spectroscopy (Model ISA J-Y U1000). The TEM samples were prepared by sonicating a small amount of the peeled CNTs in methanol for 15 min and drying a few drops of the suspension on a holey carbon or Cu grid.

## III. RESULTS

Figure 1 shows the atomic force microscopy images of the postannealed Fe samples for varying Fe thicknesses. From Figs. 1(a)–1(f), one can observe that the film thickness affects the island size, shape, and its distribution and consequently, the diameter of the nanotubes (see Table I). For an Fe film thickness of 0.5 nm, the island diameters ranged from 10 to 15 nm, for the 5-nm-thick Fe film the island diameters varied in the range of 60–120 nm, and for the 20-nm Fe film, the island diameters ranged from 200 to 600 nm. Our results indicate that the larger film thickness leads to a larger island size, which is in agreement with

TABLE I. Variation of the catalyst island size and nanotube diameter with Fe film thickness.

Fe film thickness (nm)	Island size ( $\sim$ nm)	Nanotube diameter ( $\sim$ nm)
20	200–600	100–300
10	100–200	30–120
5	60–120	30–100
2	30–60	15–30
1	30–50	5–15
0.3–0.5	10–15	1–5

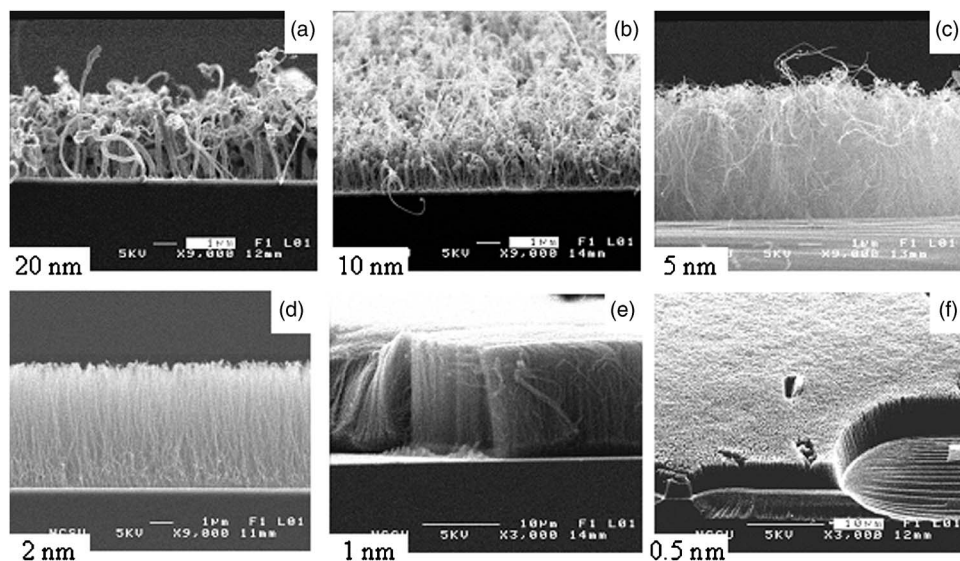


FIG. 2. Scanning electron micrograph of vertically aligned CNT films grown on different thickness Fe catalyst layers. As the Fe film thickness decreases, the diameter of the nanotubes is reduced, the areal density is increased, and the CNTs show improved alignment.

the result by Bower *et al.*<sup>13</sup> The nanotube films grown on these substrates showed a correlation of the nanotube diameter and the island size (Table I). The results indicate that the nanotube diameter is smaller than the size of the Fe catalyst islands.

SEM images of vertically aligned CNT films on different thickness Fe catalyst layers exhibit an apparent morphological variation as shown in Fig. 2. The diameters of the nanotubes decrease as the Fe film thickness is reduced from 20 to 1 nm. Figure 2(a) indicates that nanotubes grown from the 20-nm Fe layer appear fiberlike with large diameters which ranged from 100 to 300 nm. For the CNT film grown from 10-nm Fe, the structure appears to be similar to the 20-nm film showing complicated surface morphology (*a*-C and more protruded tubes), and the diameter ranged between 30 and 120 nm. Figures 2(c)–2(e) show carbon nanotube films grown from 5-, 2-, and 1-nm Fe catalyst layers where the CNTs have diameters in the range of 30–60, 10–30, and 5–15 nm, respectively. Figure 2(f) shows vertically aligned CNT films grown from 0.5-nm Fe, where a dense film with an areal density of  $\sim 10^{12}/\text{cm}^2$  was obtained.

In order to investigate how the Fe thickness affects the internal structure of the CNTs, the same sequence of CNT films shown in Fig. 2 was characterized by HRTEM [see Figs. 3(a)–3(f)]. Two important points to be noticed from these figures are (i) the increasing number of walls (from single and double to multi-) and (ii) the variation of the internal structure (from hollow to bamboolike). Figures 3(a) and 3(b) present HRTEM images of the CNTs grown from 0.3- and 0.5-nm Fe layers, respectively, where the nanotubes are either isolated or loosely bundled and are primarily hollow single- and double-wall CNTs with an average diameter of 5 nm. Figure 3(c) shows the CNTs grown from 1-nm Fe, which are double-wall and a few-wall (multiwall) as indicated by white and black arrows, respectively. The former have an average diameter of 5 nm, while the latter are  $\sim 10$  nm, and the number of tube walls is about four. Notice that all tubes exhibit a hollow structure. The film grown from 2-nm Fe has CNT with four or more walls [Fig. 3(d)]. The CNTs grown from the 5-nm Fe layer are shown in the left

and right images in Fig. 3(e). The CNT on the left displays 13 walls (each wall thickness is  $\sim 0.4$  nm) with a diameter of  $\sim 15$  nm, and the one on the right has a diameter of  $\sim 30$  nm and approximately 30 walls. The smaller nanotube [Fig. 3(e)] is hollow and exhibits parallel tubes (i.e., good crystallinity) with a small amount of *a*-C deposited on the outer walls. The larger nanotube [Fig. 3(e) right] displays a periodic bamboolike structure with one or two interlayer(s). Figure 3(f) shows the CNTs grown from 10- and 20-nm Fe layers on the left and the right of the image, respectively. The nanotube formed on the 10-nm Fe layer has a diameter of  $\sim 80$  nm and exhibits a bamboolike structure with approximately two interlayers separating the tube into many compartments. A nanotube formed on the 20-nm Fe layer resembles a fiber and has more than a few hundred walls and a diameter of  $\sim 250$  nm. The interlayers inside the nanotube almost fill the entire inside space.

The variation of growth rate with respect to Fe thickness is shown in Fig. 4(a). The growth rate for each sample was determined from the measured film thickness divided by the growth time. The uncertainty represents the variation in the thickness of the sample. The plot is subdivided into three regions (I, II, and III), which relate to the internal structure of the CNT. Below 2 nm, the CNTs are primarily hollow (I), while for an Fe thickness larger than 5 nm, the CNTs observed to have an all bamboolike internal structure (III). Between these limits, the films have CNTs which exhibit either bamboo or hollow internal structures (II). Figure 4(b) shows a schematic of the internal structure transition from hollow to bamboolike as noted in Fig. 4(a). An interesting observation is that smaller-diameter CNTs (single and double walled) exhibited an almost ten times higher growth rate than the larger-diameter multiwall nanotubes prepared under the same growth conditions.

## IV. DISCUSSION

### A. Surface versus bulk diffusion

Prior studies of carbon filament growth by Baker *et al.* have noted an Arrhenius dependence for carbon filament



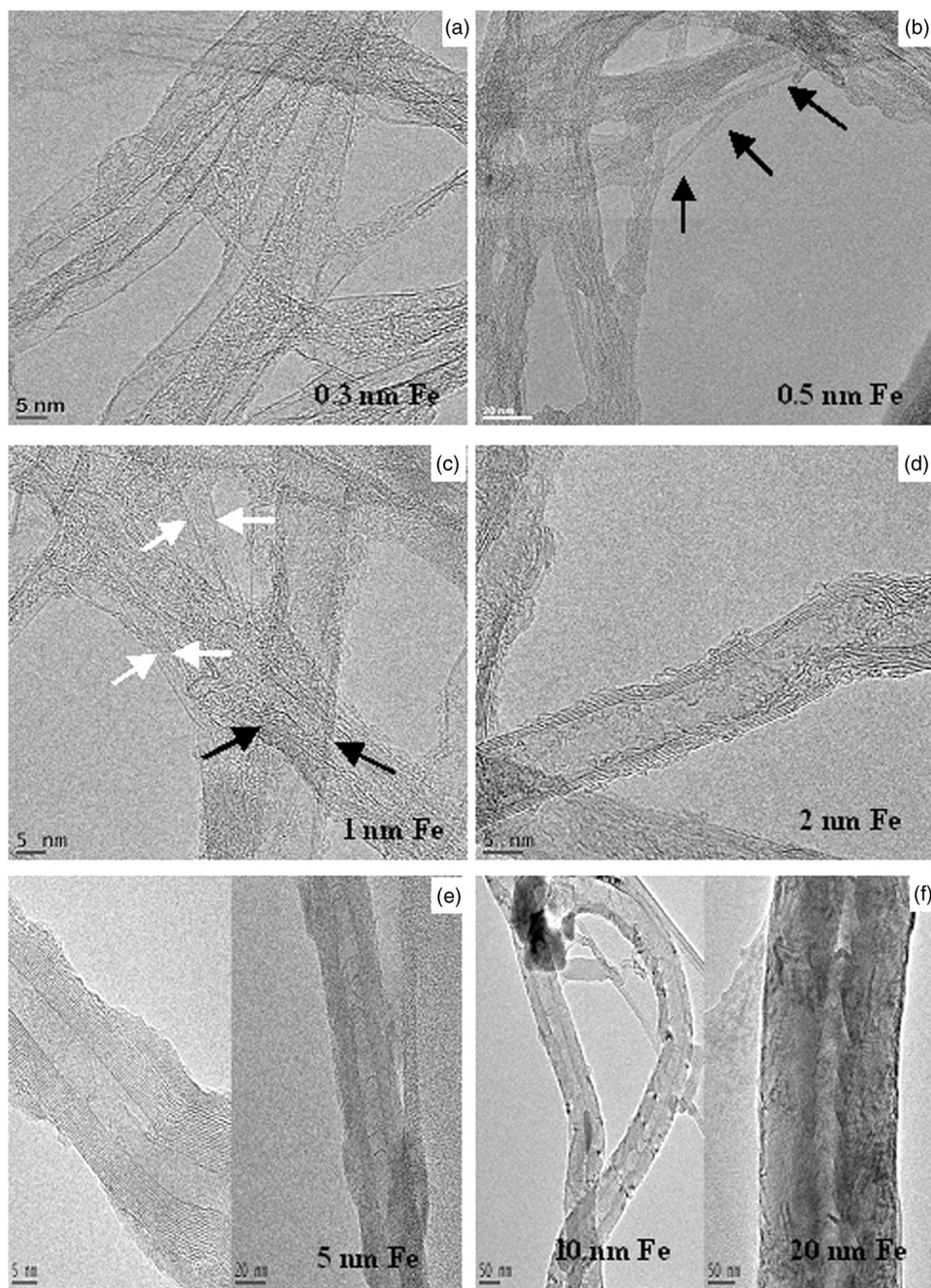


FIG. 3. HRTEM of carbon nanotubes grown from 0.3- to 20-nm Fe catalyst layers, (a)–(f). As the Fe film thickness increases, the number of walls increases from single- and double- to multiwall, and an internal structure transition (from hollow to bamboo-like) is observed. Note that the scale bars are (a) 5 nm, (b) 20 nm, (c) 5 nm, (d) 5 nm, (e) left 5 nm, (e) right 20 nm, (f) 50 nm.

growth on a transition-metal catalyst.<sup>14,15</sup> It has been established that the activation energy of the carbon filament growth was similar to the activation energy of carbon bulk diffusion in the transition-metal catalyst.<sup>15</sup> This fact also suggests that bulk diffusion may be the rate-limiting step for CNT growth. The growth mechanism for CNTs has been proposed as a combination of the following steps: diffusion of carbon into, saturation of, and precipitation out of the catalyst particles.

As far as the internal structure of the tubes is concerned, bamboo-like structure has often been observed for MWNTs grown by MWCVD, but the understanding of the origin of the internal layers, which separate the tube body into several compartments, is still rudimentary. It has been suggested that the bamboo structures might be due to the (i) catalyst particle size and shape, (ii) the slow displacement of the catalyst

compared to the growth rate of the CNTs, and (iii) bulk diffusion of carbon in the catalyst.<sup>8,10,11</sup> We showed in a previous study that the bulk diffusion of carbon is a significant factor in the formation of the bamboo-like structures. In addition to bulk diffusion, there is another path for carbon atoms to transport to the growth edge. Carbon can diffuse along the surface of the catalyst to the growth edge and then be incorporated into the nanotubes. Surface diffusion (i.e., grain-boundary diffusion) is typically a faster process compared to bulk diffusion due to the lower activation energy for surface diffusion.<sup>16</sup>

## B. Proposed growth mechanisms

We discuss the nanotube growth mechanisms in terms of surface and bulk diffusions of carbon. A schematic of this

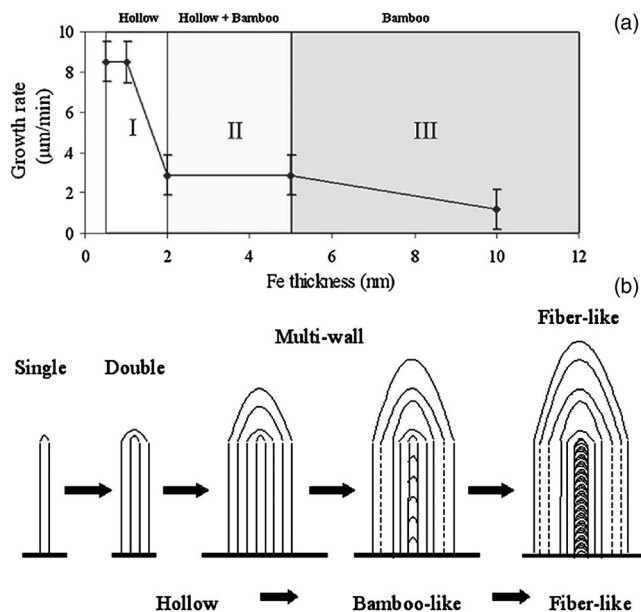


FIG. 4. (a) Plot of the CNT film growth rate vs Fe thickness where three regions (I, II, and III) with different internal structures are observed. (b) A schematic of the internal structure transition from hollow to bamboolike.

process is shown in Fig. 5. The dashed line represents the base of the nanotube, and the shaded area denotes the projection of the cross-section area of the CNT. Within this description, carbon diffuses (i) across its circumference via surface diffusion for nanotube wall formation and (ii) through the cross-sectional area via bulk diffusion to the top surface of the catalyst for wall and internal-layer formation.

For smaller-diameter catalyst particles, surface diffusion is projected as the origin of CNT walls, while for larger catalyst particles surface diffusion may combine with bulk diffusion as the source of wall formation. Bulk diffusion is projected as the primary source for the growth of the internal

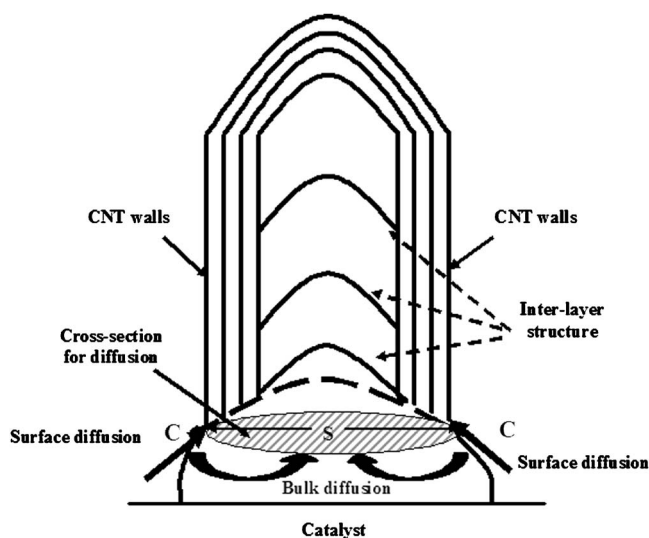


FIG. 5. A schematic of the growth model based on surface and bulk diffusions. The dashed line represents the growth edge of the nanotube, and the shaded circle denotes a cross section, where carbon diffuses: (i) across its circumference via surface diffusion for nanotube wall formation and (ii) through the cross-sectional area via bulk diffusion to the top surface of the catalyst for internal-layer formation.

structures in characteristic bamboolike CNTs.<sup>11</sup> Our model argues that depending upon the competition between surface and bulk diffusions—critically governed by catalyst particle size—different CNT structures can be synthesized. For instance, a hollow structure would be formed for smaller-diameter CNTs nucleated on small particles because surface diffusion predominates. While for larger tubes ( $>100$  nm) nucleated on larger particles, where surface and bulk diffusions may be comparable, only characteristic bamboolike structures would be anticipated. Between these extremes, both hollow and bamboolike structures would be expected.

Similar to the experiments reported by Baker *et al.*,<sup>15</sup> Hofmann *et al.*<sup>17</sup> and Ducati *et al.*<sup>18</sup> measured the growth rate of nanotubes synthesized by plasma-enhanced CVD (PECVD) using a Ni catalyst. They derived the activation energy from the growth rate to be between  $\sim 0.23$  and  $0.76$  eV. It was found that the lower bound of these values is quite close to the surface diffusion activation energy value which is  $\sim 0.3$  eV,<sup>19</sup> but much less than that of bulk diffusion activation energy of  $\sim 1.51$  eV.<sup>20</sup> Their results provide direct support to the proposed mechanism, where surface diffusion is presumed to be the major contribution for the CNT wall growth.

For our deposition conditions, the transition occurs for an Fe layer thickness between 2 and 5 nm. For Fe layer thickness beyond the transition point, all of the CNTs have bamboolike structures. Finally, when the catalyst particle size is large enough, carbon fiberlike structures appear, and in our experiments this internal structure is observed at a catalyst layer thickness of 20 nm.

It is known that CNT growth by chemical-vapor deposition is a complicated process. Our approach suggests that controlling the catalyst particle size affects the relative bulk and surface diffusion aspects. Alternatively, the surface and bulk diffusions can also be affected by surface chemistry. A study reported by Lee *et al.*<sup>21</sup> observed a decrease in the compartment distance of the bamboolike structures when nitrogen was incorporated in the gas phase. Among other effects, they suggested that nitrogen influenced the surface diffusion rates which affected the internal CNT structure. Other factors such as deposition pressure and temperature,<sup>22</sup> the shape of the catalyst, and the sticking coefficient of atoms on the catalyst surface are involved in the growth process, and they should be included in models while predicting the contributions of surface and bulk diffusion.

## V. CONCLUSION

In summary, diameter-controlled vertically aligned carbon nanotube films were synthesized by microwave plasma chemical-vapor deposition. Through continuous reduction of the thickness of the iron films, single- and double-wall nanotubes were obtained in contrast with the multiwall nanotubes and nanofibers, which were grown using a larger Fe layer thickness. The results established regimes of catalyst layer thickness where the nanotubes were hollow, bamboolike, and fiberlike. A simple model was proposed which described the growth in terms of surface and bulk diffusion. It established that the transition in structure could be critically governed by

the size of the catalyst particle. Due to the competition between these two processes during growth of nanotubes, diverse internal structures are observed, and we proposed that surface diffusion predominates for thin catalyst layers resulting in hollow and small-diameter nanotubes, while for thicker catalyst layers, bulk diffusion becomes more significant and multiwall, large-diameter nanotubes are formed with bamboolike internal structures.

## ACKNOWLEDGMENTS

This research work is supported in part by the ONR through the TEC-MURI and the DOE through the ANL CESP program.

<sup>1</sup>H. Dai, *Surf. Sci.* **500**, 218 (2002).

<sup>2</sup>P. J. F. Harris, *Carbon Nanotubes and Related Structures* (Cambridge University Press, London, 1999).

<sup>3</sup>A. M. Fennimore, T. D. Yuzvinsky, W. Han, M. S. Fuhrer, J. Cumings, and A. Zettl, *Nature (London)* **424**, 408 (2003).

<sup>4</sup>W. Huang, S. Fernando, L. F. Allard, and Y. P. Sun, *Nano Lett.* **3**, 565 (2003).

<sup>5</sup>J. M. Bonard, K. A. Dean, B. F. Coll, and C. Klinke, *Phys. Rev. Lett.* **89**, 197602 (2002).

<sup>6</sup>K. B. K. Teo, C. Singh, M. Chhowalla, and W. I. Milne, *Encyclopedia of Nanoscience and Nanotechnology*, edited by H. S. Nalwa (American Sci-

entific Publishers, Stevenson Ranch, CA, 2003), Vol. X, pp. 1–22.

<sup>7</sup>Y. Y. Wang, G. Y. Tang, F. A. M. Koeck, B. Brown, J. M. Garguilo, and R. J. Nemanich, *Diamond Relat. Mater.* **13**, 1287 (2004).

<sup>8</sup>L. Yuan, T. Li, and K. Saito, *Carbon* **41**, 1889 (2003).

<sup>9</sup>C. Ducati, I. Alexandrou, M. Chhowalla, J. Robertson, and G. A. J. Amaratunga, *J. Appl. Phys.* **95**, 6387 (2004).

<sup>10</sup>V. V. Kovalevski and A. N. Safronov, *Carbon* **36**, 963 (1998).

<sup>11</sup>C. J. Lee and J. Park, *Appl. Phys. Lett.* **77**, 3397 (2000).

<sup>12</sup>F. A. M. Kock, J. M. Garguilo, and R. J. Nemanich, *Diamond Relat. Mater.* **10**, 1714 (2001).

<sup>13</sup>C. Bower, O. Zhou, W. Zhu, D. J. Werder, and S. Jin, *Appl. Phys. Lett.* **77**, 2767 (2000).

<sup>14</sup>R. T. K. Baker, P. S. Harris, R. B. Thomas, and R. J. Waite, *J. Catal.* **30**, 86 (1973).

<sup>15</sup>R. T. K. Baker, J. J. Chludzinski, N. S. Dudash, and A. Simoens, *Carbon* **21**, 463 (1983).

<sup>16</sup>P. Shewmon, *Diffusion in Solids, A Publication of The Minerals & Materials Society*, Pennsylvania, 1999).

<sup>17</sup>S. Hofmann, C. Ducati, and J. Robertson, *Appl. Phys. Lett.* **83**, 135 (2003).

<sup>18</sup>C. Ducati, L. Alexandrou, M. Chhowalla, G. A. J. Amaratunga, and J. Robertson, *J. Appl. Phys.* **92**, 3299 (2002).

<sup>19</sup>J. F. Mojica and L. L. Levenson, *Surf. Sci.* **59**, 447 (1976).

<sup>20</sup>S. Diamond and C. Wert, *Trans. AIME* **239**, 705 (1967).

<sup>21</sup>C. J. Lee, S. C. Lyu, H.-W. Kim, J. H. Lee, and K. I. Cho, *Chem. Phys. Lett.* **359**, 115 (2002).

<sup>22</sup>J.-M. Bonard, M. Croci, C. Klinke, F. Conus, I. Arfaoui, T. Stockli, and A. Chatelain, *Phys. Rev. B* **67**, 085412 (2003).